Title
A Distinct Inhibitory Function for miR-18a in Th17 Cell Differentiation

Journal
The Journal of Immunology, 199(2)

ISSN
0022-1767

Authors
Montoya, Misty M
Maul, Julia
Singh, Priti B
et al.

Publication Date
2017-07-15

DOI
10.4049/jimmunol.1700170

Peer reviewed

Published in final edited form as:

J Immunol. 2017 July 15; 199(2): 559–569. doi:10.4049/jimmunol.1700170.

A distinct inhibitory function for miR-18a in Th17 cell differentiation[1]

Misty M. Montoya[*], **Julia Maul**[†], **Priti B. Singh**[*], **Heather H. Pua**[‡], **Frank Dahlström**[†], **Nanyan Wu**[§], **Xiaozhu Huang**[§], **K. Mark Ansel**[2,*,¶], and **Dirk Baumjohann**[2,†,¶]

[*]Department of Microbiology & Immunology, Sandler Asthma Basic Research Center, University of California San Francisco, San Francisco, CA 94143, USA

[†]Institute for Immunology, Biomedical Center Munich, Ludwig-Maximilians-Universität München, Grosshaderner Str. 9, 82152 Planegg-Martinsried, Germany

[‡]Department of Pathology, University of California, San Francisco, San Francisco, CA, USA

[§]Lung Biology Center, Department of Medicine, University of California San Francisco, San Francisco, California, USA

Abstract

T helper (Th)17 cell responses orchestrate immunity against extracellular pathogens, but also underlie autoimmune disease pathogenesis. Here, we uncovered a distinct and critical role for miR-18a in limiting Th17 cell differentiation. miR-18a was the most dynamically upregulated miRNA of the miR-17~92 cluster in activated T cells. miR-18a deficiency enhanced $CCR6^{+}ROR\gamma t^{+}$ Th17 cell differentiation *in vitro* and increased the number of tissue Th17 cells expressing CCR6, RORγt and IL-17A in airway inflammation models *in vivo*. Sequence-specific miR-18 inhibitors increased CCR6 and RORγt expression in both mouse and human $CD4^{+}$ T cells, revealing functional conservation. miR-18a directly targeted *Smad4*, *Hif1a*, and *Rora*, all key transcription factors in the Th17 cell gene expression program. These findings indicate that activating signals influence the outcome of T helper cell differentiation via differential regulation of mature miRNAs within a common cluster.

[1]This work was supported by the US National Institutes of Health grants (R01HL109102, P01HL107202, U19CA179512, F31HL131361), a Leukemia & Lymphoma Society scholar award (K.M.A.), the National Institute of General Medical Sciences (NIGMS) Medical Scientist Training Program (Grant #T32GM007618) (M.M.), the National Multiple Sclerosis Society, the UCSF Program for Breakthrough Biomedical Research, funded in part by the Sandler Foundation, and the Deutsche Forschungsgemeinschaft (Emmy No ether Programme BA 5132/1-1 and SFB 1054 Teilprojekt B12) (D.B.).

[2]Address correspondence and reprint requests to Dr. Dirk Baumjohann, Institute for Immunology, Biomedical Center Munich, Ludwig-Maximilians-Universität München, Grosshaderner Str. 9, 82152 Planegg-Martinsried, Germany, dirk.baumjohann@med.uni-muenchen.de, tel +49-89-2180-75660, fax +49-89-2180-9975660) or Dr. K. Mark Ansel, Department of Microbiology & Immunology, Sandler Asthma Basic Research Center, University of California San Francisco, San Francisco, CA 94143, USA, mark.ansel@ucsf.edu, tel 415-476-5368, fax 415-502-4995).

[¶]Equal contribution

Author contributions: M.M. performed and analyzed most of the experiments under the supervision of K.M.A. and D.B.; J.M., P.B.S., H.H.P., F.D., N.W., X.H., and D.B. performed and analyzed some of the experiments. M.M., K.M.A., and D.B. designed the experiments, interpreted the data, and wrote the manuscript.

Disclosures: The authors have no financial conflicts of interest.

Introduction

T helper (Th) cells orchestrate cellular and antibody-mediated immunity against a variety of pathogens. To accommodate this functional diversity, Th cells differentiate into distinct subsets classified by defined phenotypic characteristics and specialized functions in immunity (1). Th17 cells combat extracellular bacteria and fungi, but they have also been implicated in the pathogenesis of several autoimmune and inflammatory diseases, including multiple sclerosis and psoriasis (2-4). Th17 cells also mediate immune responses that are involved in maintaining epithelial barrier integrity, and it has been widely suggested that some cases of asthma may be caused by dysregulated Th17 responses (4, 5). Studies of both human asthma and mouse models indicate that lung inflammation can shift to a response marked by Th17 cytokines and neutrophil infiltration when Th2 cell-mediated eosinophilia is reduced (6, 7). Understanding how Th17 cells are programmed and contribute to tissue inflammation remains an important research frontier with high potential for therapeutic impact in a broad spectrum of inflammatory diseases.

Th17 cells can be generated *in vitro* by activating $CD4^+$ T cells in the presence of TGFβ and IL-6 (8-10). They are characterized by IL-17 secretion and expression of their lineage-defining transcription factor, RAR-related orphan receptor (ROR)γt. The closely related factor RORα is also an important transcriptional regulator of the Th17 gene expression program (11). Th17 cells are commonly identified by expression of the RORγt/RORα target gene *Ccr6*, which encodes a chemokine receptor important for Th17 cell trafficking into the brain and mucosal tissues (12-15). In addition to RORγt and RORα, Th17 cells utilize multiple additional transcription factors in a robust transcriptional network that promotes their gene expression program (16, 17). Of note, HIF1α is a limiting factor that regulates Th17 cell biology (18-20), and SMAD4 cooperates with SMAD2/3 to transduce TGFβ signaling in differentiating Th17 cells.

MicroRNAs (miRNAs) have emerged as potent regulators of T helper cell differentiation, function and plasticity (21). MicroRNAs are small endogenously expressed RNAs that regulate gene expression at the post-transcriptional level. Individual miRNAs can target hundreds of distinct mRNAs, and each mRNA can have several miRNA binding sites. Th17 cell differentiation is impaired in miRNA-deficient T cells (22), and important roles have been identified for several particular miRNAs (18, 23, 24). Some of these miRNAs indirectly influence Th17 lineage commitment by acting on other cell types (25), while others act directly on cell-intrinsic signaling that induces Th17 cell programming, expansion and effector function *in vitro* and in mouse models of autoimmunity (18, 25-29).

The *Mirc1* locus, better known as the miR-17~92 cluster, encodes six miRNAs in four families (miR-17, miR-18, miR-19, and miR-92 families), each defined by a common ‘seed sequence’ and predicted target genes (30). The miR-17~92 cluster and miRNAs in these four families are important for T cell proliferation and survival, and for the proper differentiation and immunological functions of Treg, Tfh, Th1, Th2 and Th17 cells (21, 31-41). In Tfh cells, miR-17~92 deficiency also induced inappropriate expression of Th17-associated genes (34). Studies that dissected the functionally relevant miRNAs within the miR-17~92 cluster in T cells have focused almost entirely on the miR-17 and miR-19

families, and uncovered similar roles in promoting clonal expansion and cytokine production in a variety of Th subsets (31, 32, 35, 40, 41). In contrast, miR-18a has drawn little attention. No unique function has been ascribed to this miRNA in immune cells, and recently characterized miR-18a-deficient mice did not show any overt immunopathological features (42).

Here, we uncovered a unique role for miR-18a as a highly inducible inhibitor of Th17 differentiation. Accordingly, miR-18a-deficient mice exhibited increased Th17 responses in airway inflammation models *in vivo*. We identified *Smad4*, *Hif1a*, and *Rora* as important target genes mediating miR-18a regulation of Th17 cell differentiation.

Materials and methods

Mice

Mice with *lox*P sites flanking the miR-17~92 cluster (*Mirc1*$^{tm1.1Tyj}$; The Jackson Laboratory, 008458) were crossed to CD4-Cre mice (*Tg(CD4-cre)1Cwi;* Taconic, 4196) to generate T cell-specific miR-17~92-deficient mice. For some experiments, these mice were further crossed with *Smad4*$^{tm2.1Cxd}$ mice containing loxP sites flanking exon 8 of the *Smad4* gene (The Jackson Laboratory, 017462) or with mice heterozygous for the spontaneous *Rora*^{sg} mutation (The Jackson Laboratory, 002651) to generate miR-17~92-deficient mice with heterozygous deletion of *Smad4* or with one defective *Rora* allele and appropriate littermate controls. Mice with a targeted deletion of miR-18a (*Mir18*$^{tm1.1Aven}$) were recently described (42). Mice with *lox*P-flanked *Dgcr8* alleles (*Dgcr8*$^{tm1.1Blel}$) have been described before (43) and were bred to CD4-Cre and R26-stop-EYFP mutant mice (*Gt(ROSA)26Sor*$^{tm3(CAG-EYFP)Hze}$*;* The Jackson Laboratory, 006148). All mice were housed and bred in the specific pathogen-free barrier facilities at the University of California San Francisco or the Ludwig-Maximilians-Universität München. All experiments were performed according to the Institutional Animal Care and Use Committee (IACUC) guidelines of the University of California, San Francisco, or in accordance with the regulations of the Regierung von Oberbayern.

In vitro mouse primary T cell polarization

Single-cell suspensions from spleen and lymph nodes were prepared by mincing the tissues between the frosted ends of glass slides. Cells were filtered through fine mesh and counted. $CD4^+$ T cells were enriched with the Easy Sep Mouse $CD4^+$ T Cell Isolation Kit (Stemcell Technologies). Purified $CD4^+$ T cells were plated at 4×10^6 cells per well in complete medium (RPMI-1640 supplemented with 10% fetal bovine serum, pyruvate, nonessential amino acids, l-arginine, l-asparagine, l-glutamine, folic acid, beta mercaptoethanol, penicillin and streptomycin) in 6-well plates (Corning Costar) or 1×10^5 cells per well in 96-well, flat-bottom plates (Corning Costar) pre-coated with 2μg/ml anti-CD3 (clone 17A2; Bio X Cell) and anti-CD28 (clone 37.51; Bio X Cell). For Th17 polarizing conditions, media were supplemented with anti-IFNγ (10μg/ml, clone XMG1.2; Bio X Cell), anti-IL-4 (10μg/ml, clone 11B11; Bio X Cell), human TGFβ (5ng/ml; Peprotech), and murine IL-6 (25ng/ml; Peprotech), unless otherwise stated. In one condition of the TGFβ dosing experiments, no exogenous TGFβ was added to the culture and cell-derived TGFβ was

blocked with anti-TGFβ (20μg/ml, clone 1D11; Bio X Cell). On day 2 of culture, cells were collected, counted, suspended in transfection buffer together with miRNA mimics, siRNAs or inhibitors, and transfected with the Neon transfection system (Invitrogen). Cells were immediately transferred into fresh culture medium containing Th17-polarizing cytokines plus murine IL-23 (20ng/ml; R&D Systems) at 4×10^5 cells per well in 96-well flat-bottom plates pre-coated with anti-CD3 and anti-CD28. Cultured cells were usually analyzed on day 3.5 of initial culture unless otherwise stated.

In vitro human cord blood T cell polarization

Cord blood mononuclear cells (CBMCs) from anonymous human cord blood donors were isolated by Lymphoprep gradient (1114545; Accurate Chemical & Scientific). $CD4^+$ T cells were isolated from CBMCs using the Dynabeads Untouched Human $CD4^+$ T Cell Isolation Kit (Invitrogen). Cells were stimulated for ~48 h on plates coated with 2μg/ml anti-CD3 (clone OKT-3; UCSF Monoclonal Antibody Core) and 4μg/ml anti-CD28 (clone 15E8; Miltenyi Biotec) at an initial density of $4\text{-}5\times10^6$ cells per well in complete medium (RPMI-1640 media with 10% FCS, pyruvate, nonessential amino acids, l-arginine, l-asparagine, l-glutamine, folic acid, beta mercaptoethanol, penicillin and streptomycin) in 6-well plates (Corning Costar). After 2 days of stimulation, cells were collected, counted, suspended in transfection buffer together with miRNA inhibitors, and transfected with the Neon transfection system (Invitrogen). Cells were immediately transferred into 48-well plates at a density of 4×10^5 cells per well pre-coated with anti-CD3 and anti-CD28 in fresh culture medium containing Th17-polarizing cytokines. For Th17-polarizing conditions, media were supplemented with anti-human IFNγ (10μg/ml, clone NIB42; eBioscience), anti-human IL-4 (10μg/ml, clone MP4-25D2; Biolegend), human TGFβ (5ng/ml; Peprotech), human IL-6 (25ng/ml; Peprotech), human IL-1β (20ng/ml; Peprotech), and human IL-23 (20ng/ml; Peprotech).

miRNA mimics, miRNA inhibitors, siRNAs, and miRNA sensors

Th17-polarized human or mouse primary $CD4^+$ T cells were transfected with miRNA mimics, siRNAs or inhibitors at 48 h of cell culture with the Neon Transfection System (Invitrogen) as previously described (41). miRIDIAN miRNA mimics (Dharmacon) or siGENOME SmartPools (Dharmacon) were used at 500nM and miRCURY LNA microRNA Power family inhibitors (Exiqon) were used at 5μM or 20μM with appropriate controls. MSCV-PGK-hCD25 miRNA sensors for miR-17, miR-18a, miR-92a, and miR-19b (Simpson et al., 2014) were constructed to express EGFP with four perfectly complementary binding sites for the miRNA of interest in the 3′UTR as previously described (41). Cells were transduced by spin infection early on day 2 of Th17 cultures and transfected with miRNA mimics or inhibitors later on day 2 of Th17 cultures. $hCD25^+$ $CD4^+$ T cells were analyzed on day 3.5 for EGFP expression.

3′UTR cloning and Luciferase assays

3′UTR dual luciferase plasmids containing near full length 3′UTRs of *Smad4*, *Hif1a* or an extension 3′UTR for *Smad4* were cloned into the psiCHECK-2 luciferase reporter construct (Promega). Primer sequences were: *Smad4* F: TAGTAGCTCGAGCTCTGCAGCTCTTGGATGAA, *Smad4* R:

TAGTAGGCGGCCGCCATGGGAAAGTCCTGGTAGAG, *Hif1a* F: TAGTAGCTCGAGGGCAGCAGAAACCTACTGCAGG, *Hif1a* R: TAGTAGGCGGCCGCTAAACGTAAGCGCTGACCCAGG, *Smad4* extension F: TAGTAGCTCGAGACTGAGTCACTATACGAAGTGG, *Smad4* extension R: TAGTAGGCGGCCGCTTGGCTCTGAAGAGATACTTCC. psiCHECK-2 *Rora* 3′UTRP1 was described previously (34). $CD4^+$ T cells were transfected on day 2 of ThN (non-polarizing, no exogenous cytokines or blocking antibodies) culture with luciferase reporter constructs and/or miRNA mimics using the Neon Transfection System. Media were additionally supplemented with 20 units/ml recombinant human IL-2 (NCI) on day 2 of culture. Luciferase activity was measured 24 h after transfection with the Dual Luciferase Reporter Assay System (Promega) and a FLUOstar Optima plate-reader (BMG Labtech).

Flow cytometry

Cultured cells were collected, washed, and stained with antibodies against cell surface proteins and transcription factors as described before (44). Nonspecific binding was blocked with anti-CD16/CD32 (clone 2.4G2; UCSF Monoclonal Antibody Core), 2% normal rat/mouse serum for mouse T cell staining or with human FcR binding inhibitor (eBioscience) for human T cells. Dead cells were excluded with Fixable Viability Dye eFluor780 (eBioscience). For *in vitro* cell proliferation experiments, naive $CD4^+$ T cells were labeled with 5 μM CellTrace Violet (Invitrogen) as described before (44). The proliferation index was calculated with FlowJo software (Tree Star). For intracellular staining of transcription factors, the Foxp3 staining set (eBioscience) was used. Intracellular cytokine detection was performed after stimulation with 10nM PMA and 1μM ionomycin for 2 h, followed by the addition of 5μg/ml Brefeldin A for another 2 h. Cells were fixed with 4% PFA for 8 min at room temperature, washed with ice-cold PBS, and permeabilized with 0.5% saponin. The following fluorochrome-conjugated antibodies were used in the study for mouse T cells: anti-CD4 (clones RM4-5 or GK1.5), anti-IL-17A (eBio17B7), anti-IFNγ (XMG1.2), and anti-IL-13 (eBio13A; all from eBioscience); anti-CD11b (M1/70; Biolegend); anti-CCR6 (140706), anti-RORγt (Q31-378), anti-Siglec F (E50-2440), anti-CD45 (30-F11), anti-Ly6G (1A8; all from BD Biosciences); and for human T cells: anti-human CD4 (OKT4; Biolegend), anti-human CCR6 (R6H1; eBioscience); and anti-human RORγt (Q21-559; BD Biosciences). Apoptotic cells were quantified with the PE Annexin V Apoptosis Detection Kit I (BD Biosciences) according to the manufacturer's instructions. Samples were acquired on a LSR II or LSRFortessa cytometer (BD Biosciences) and analyzed with FlowJo software (Tree Star).

In vivo airway hypersensitivity models

Acute 10-day OVA model: Sex and age matched wildtype and miR-$18^{\Delta/\Delta}$ mice were sensitized by i.p. injection with 50μg ovalbumin (OVA, Sigma-Aldrich) in 100μl of PBS plus 100μl of Imject Alum Adjuvant (Thermo Scientific). After seven days, the mice were challenged oropharyngeally with 50μg OVA in 20μl of PBS daily for 3 consecutive days. Lungs were harvested on day 10 of the experiment. 27-day OVA+LPS model: Sex and age matched wildtype and miR-$18^{\Delta/\Delta}$ mice were sensitized with 100μg of EndoFit Ovalbumin (OVA, InvivoGen) and 10μg of LPS (Sigma-Aldrich) in 30μl of PBS delivered by oropharyngeal instillation on days 0, 2, 4, and 11. The mice were then challenged

oropharyngeally with 40μg of OVA in 30μl of PBS on days 18, 20, 25, and 26. Lungs and lung-draining mediastinal lymph nodes were harvested on day 27. For both airway hypersensitivity models, lungs were digested following the lung dissociation kit protocol and gentle MACS dissociator (Miltenyi Biotec). Liberase TM (Roche) was used at 50μg/ml and DNase I (Roche) at 25μg/ml. Cells collected from the lung and lung-draining lymph nodes were analyzed by flow cytometry for surface markers, transcription factors and cytokines as described above. Prior to euthanasia, mice were injected retro-orbitally with 2μg of fluorochrome-conjugated anti-CD45 antibody (clone 30-F11; BD Biosciences) in 200μl of PBS to distinguish vascular and non-vascular cells in the lung. Routine hematoxylin and eosin and periodic acid-Schiff (PAS) stainings were performed to assess lung inflammatory cell infiltration and metaplasia of the respiratory epithelium, respectively. A trained histopathologist scored all stained tissue sections.

qPCR

$CD4^+$ T cells from spleen and lymph nodes of mice were enriched with the EasySep Mouse $CD4^+$ T Cell Isolation Kit (Stemcell Technologies). Cells were lysed in Trizol LS (Life Technologies), total RNA was isolated, and RNA was then quantified with a ND-1000 spectrophotometer (NanoDrop). Reverse transcription of miRNA was performed with the NCode miRNA First-Strand cDNA Synthesis Kit (Life Technologies). Forward primers were the mature miRNA sequence (45) and a universal reverse primer was used from the kit. Expression values were normalized to 5.8S ribosomal RNA (F: ATCGTAGGCACCGCTACGCCTGTCTG). Reverse transcription of mRNA was performed with SuperScript III First-Strand Synthesis for RT-PCR (Invitrogen). Primers for *Smad4* total transcript were CACAATGAGCTTGCATTCCAG (F) and ACCTTAAACGTCTCTCCTACCT (R). Primers for *Smad4* extended transcript were CTGAGTCACTATACGAAGTGGAAT (F) and GTCATTTAGCAGAAGGTGTCTTG (R). Expression values were normalized to *Gapdh* (F: GTGTTCCTACCCCCAATGTGT; R:ATTGTCATACCAGGAAATGAGCTT). qPCR was performed in technical duplicates using FastStart Universal SYBR Green Master mix (Roche) on a Realplex^2 instrument (Eppendorf).

Statistics

Excel (Microsoft) and Prism (GraphPad) were used for data analysis. For all figures, bar graphs display mean+s.e.m., unless otherwise stated. Z-scores were calculated from mean and s.d.. *P<0.05, **P<0.01, and ***P<0.001 for significance. Appropriate statistical analyses were performed for all data and are specified in each corresponding figure legend.

Results

miR-18a is the most dynamically regulated miRNA of the miR-17~92 cluster during Th17 cell differentiation

The miR-17~92 cluster comprises six different miRNAs that can be grouped into four distinct families based on their seed sequence (Fig. 1A). To gain insight into the dynamics of miR-17~92 expression during Th17 cell differentiation, we first cultured purified control ($17{\sim}92^{+/+}$ = CD4-Cre^- miR-$17{\sim}92^{fl/fl}$) and miR-17~92-deficient ($17{\sim}92^{\Delta/\Delta}$ = CD4-Cre^+

miR-17~92$^{fl/fl}$) CD4$^+$ T cells *in vitro* for 4 days under classical Th17-polarizing conditions (TGFβ+IL-6). We assessed the expression of each miRNA in the miR-17~92 cluster during the course of Th17 differentiation by quantitative PCR (Fig. 1B). All of the miR-17~92 cluster miRNAs were expressed in 17~92$^{+/+}$ CD4$^+$ T cells under these conditions and, as expected, all six miRNAs were absent in 17~92$^{\Delta/\Delta}$ CD4$^+$ T cells. While most miRNAs from this cluster were induced upon activation, miR-18a was the most dynamically regulated, showing a greater than ten-fold induction that was sustained over three days in culture. Mature miR-92a was not induced together with the other cluster miRNAs. Importantly, representative miRNAs from the paralogous miRNA gene clusters miR-106b~25 and miR-106a~363 (Fig. 1A) were expressed at comparable levels in 17~92$^{+/+}$ and 17~92$^{\Delta/\Delta}$ CD4$^+$ T cells throughout the time course (Fig. 1C). Consistent with previous reports (46), miR-25 was abundant in developing Th17 cells, whereas miR-363 was barely detectable (Fig. 1C).

miR-18a is active in differentiating CD4$^+$ T cells

To assess the inhibitory activity of each miRNA family represented within the miR-17~92 cluster, we used previously developed retroviral miRNA activity sensors in developing Th17 cells (31, 41). Each reporter encodes EGFP with four binding sites for the miRNA of interest within an artificial 3′UTR, resulting in EGFP expression that is inhibited by miRNAs of the corresponding family in a sequence-specific fashion (Supplementary Fig. 1). We assessed the activity of the miR-17, miR-18, miR-19, and miR-92 families in 17~92$^{+/+}$ control and17~92$^{\Delta/\Delta}$ Th17 cells (Fig. 1D). Sensor EGFP expression was increased in 17~92$^{\Delta/\Delta}$ Th17 cells as compared to 17~92$^{+/+}$ control cells, indicating that endogenous miR-17~92 cluster miRNAs from all four families actively inhibit target mRNAs. However, the increase in EGFP expression was greatest for miR-18 and miR-19 sensors. 17~92$^{\Delta/\Delta}$ Th17 cells displayed only intermediate EGFP expression from miR-17 and miR-92 sensors, suggesting that other family members encoded outside of the miR-17~92 cluster make substantial contributions to miR-17 and miR-92 activity in Th17 cells. These findings were further corroborated by experiments with locked nucleic acid miRNA “family inhibitors”, designed to simultaneously inhibit all members of each family (Supplementary Fig. 1). The miR-17 family inhibitor further increased the already elevated miR-17 sensor EGFP expression in 17~92$^{\Delta/\Delta}$ Th17 cells. Similar results were obtained for miR-19 and miR-92 family inhibitors and matched sensors, suggesting residual activity beyond what is accounted for by miR-17~92 cluster miRNAs. In contrast, the miR-18 sensor EGFP expression was unaffected by the miR-18 family inhibitor in 17~92$^{\Delta/\Delta}$ Th17 cells. Taken together, deletion of miR-17~92 was sufficient to nearly abolish miR-18 and strongly reduce miR-19 activity, but other members of the miR-17 and miR-92 families retained substantial activity in 17~92$^{\Delta/\Delta}$ Th17 cells.

miR-18a inhibits Th17 cell differentiation

To determine the individual contribution of miR-18a and the other miR-17~92 cluster miRNAs to Th17 cell differentiation, we first cultured purified 17~92$^{+/+}$ and 17~92$^{\Delta/\Delta}$ CD4$^+$ T cells *in vitro* for 4 days under classical Th17-polarizing conditions (TGFβ+IL-6). 17~92$^{\Delta/\Delta}$ T cells showed increased expression of CCR6 and RORγt (Fig. 2A) with variable IL-17A production (Fig. 2B). To isolate individual effects of each member of the

miR-17~92 cluster on Th17 cell differentiation, miRNA mimics were transfected into activated 17~92$^{\Delta/\Delta}$ CD4^{+} T cells cultured under Th17-polarizing conditions, and the effect on CCR6, RORγt, and IL-17A expression was assessed by flow cytometry. Strikingly, only miR-18a could significantly rescue the increased frequency of CCR6^{+}RORγt^{+} cells in 17~92$^{\Delta/\Delta}$ Th17 cells, restoring it to the frequency observed in 17~92$^{+/+}$ cells (Fig. 2C). In contrast, several other miRNAs of the cluster further increased the already enhanced frequency of CCR6^{+}RORγt^{+} cells in 17~92$^{\Delta/\Delta}$ Th17 cell cultures (Fig. 2C). Consistent with a previous report (32), miR-17 family members also enhanced IL-17 production (Supplementary Fig. 2). These data demonstrate that miR-18a exhibits a distinct inhibitory function on CCR6^{+}RORγt^{+}Th17 cells.

Genetic ablation of miR-18a alone increases the frequency of CCR6^{+}RORγt^{+} Th17 cells

To directly assess the requirement for endogenous miR-18a, we tested Th17 differentiation in miR-18$^{\Delta/\Delta}$ CD4^{+} T cells from recently developed mice that harbor a targeted deletion of miR-18 while retaining normal expression of all the remaining miR-17~92 miRNAs (42). Similar to what we observed for miR-17~92 cluster deletion, loss of miR-18a alone increased the frequency of CCR6^{+} and CCR6^{+}RORγt^{+} cells among cultured Th17 cells, with no consistent effect on RORγt expression (Fig. 3A) or IL-17 production (Fig. 3B). These defects could be rescued by transfecting a miR-18a mimic into miR-18$^{\Delta/\Delta}$ CD4^{+} T cells (Fig. 3C). Since miR-17~92-deficiency considerably impairs CD4^{+} T cell proliferation, expansion, and survival (21), we next analyzed if miR-18-deficiency impacted these processes as well. Importantly, we did not observe any differences in the proliferative capacity of miR-18$^{\Delta/\Delta}$ CD4^{+} T cells as compared to WT control cells (Fig. 3D). In addition, we did not detect any changes in the rate of apoptotic cells under these culture conditions (Fig. 3E). Taken together, these data demonstrate that miR-18a plays a critical role in limiting Th17 cell differentiation *in vitro*.

miR-18a deficiency increases lung Th17 cell frequencies in airway inflammation models

Next, to test the requirement of endogenous miR-18a for Th17 responses *in vivo*, we induced asthma-like inflammation in the lungs of control and miR-18$^{\Delta/\Delta}$ mice by sensitizing/challenging these mice with ovalbumin (OVA) (Fig. 4A). While we observed no differences in the numbers of CD4^{+} T cells or overall CD45^{+} leukocytes (Fig. 4B), frequencies of CCR6^{+} and CCR6^{+}RORγt^{+} CD4^{+} T cells were significantly increased in miR-18$^{\Delta/\Delta}$ mice (Fig. 4C). This was also reflected in elevated RORγt gMFI of miR-18$^{\Delta/\Delta}$ CD4^{+} T cells compared to miR-18$^{+/+}$ CD4^{+} T cells. Importantly, frequencies of IL-17-producing cells were also significantly increased among re-stimulated miR-18-deficient lung CD4^{+} T cells, while frequencies of IL-13-producing Th2 cells and IFNγ-producing Th1 cells were not affected (Fig. 4D). The number of lung eosinophils, but not neutrophils, was decreased (Fig. 4E), consistent with a shift from Th2-mediated to Th17-mediated inflammation (47) in miR-18$^{\Delta/\Delta}$ airways. We also determined the *in vivo* function of miR-18 in an inhaled LPS+OVA model of airway inflammation (Fig. 4F). In this model, miR-18 deficiency also increased Th17 cells in the lung without affecting IL-13 producing Th2 cells and IFNγ-producing Th1 cells (Fig. 4G, H). Histologic sections showed dense inflammation surrounding vessels and conducting airways in the lungs of both control and miR-18$^{\Delta/\Delta}$ mice (Fig. 4I). However, consistent with a shift from Th2-mediated to Th17-mediated

inflammation, miR-18$^{\Delta/\Delta}$ mice showed significantly less mucus-producing lung airway epithelium (Fig. 4J). Finally, miR-18 deficiency also increased Th17 cells in the lung-draining mediastinal lymph nodes (Fig. 4K).

Inhibition of the miR-18 family increases mouse and human Th17 cell differentiation

The ability to specifically inhibit miRNAs from the miR-17~92 cluster in a family-wise manner using transfectable inhibitors gave us the opportunity to test whether endogenous miR-18 is important for Th17 differentiation. In line with the observed increase in CCR6^{+}RORγt^{+} Th17 cell differentiation of miR-18a-deficient cells *in vitro* (Fig. 3) and *in vivo* (Fig. 4), inhibition of the miR-18 family significantly increased the expression of CCR6 and RORγt in both mouse and human Th17 cells (Fig. 5A and B, respectively). These data indicate that miR-18 acts as an evolutionarily conserved inhibitor of Th17 cell differentiation. Our miRNA family inhibitor experiments also confirmed the miR-17 family's role in promoting cytokine production (32), as the miR-17 family inhibitor reduced IL-17 production in transfected Th17 cells (Supplementary Fig. 2).

Smad4, *Hif1a,* and *Rora* are functionally relevant direct miR-18a target genes

To identify relevant miR-18a target genes in Th17 cell differentiation, we compiled a list of 18 previously reported miR-18 family target genes from miRTarBase (48) and performed siRNA-mediated inhibition of these genes in 17~92$^{\Delta/\Delta}$ CD4^{+}T cells to determine whether any of them are limiting factors for *in vitro* Th17 cell differentiation and effector cytokine production. siRNA SmartPools against several of these genes altered the expression of CCR6, RORγt and/or IL-17 (Supplementary Fig. 3). Following retesting with siRNA SmartPools to confirm effects observed in the primary screen (data not shown), the top five target genes whose pooled siRNAs at least partially rescued the increased CCR6 and/or RORγt expression of 17~92$^{\Delta/\Delta}$ CD4^{+} T cells were examined further. To this end, 17~92$^{\Delta/\Delta}$ CD4^{+} T cells were separately transfected with three individual unique siRNAs against each gene (Fig. 6A). Multiple siRNAs against *Smad4*, a transcriptional mediator of TGFβ signaling, reversed the exaggerated increase in CCR6^{+}RORγt^{+} 17~92$^{\Delta/\Delta}$ T cells. The siRNA SmartPool against *Hif1a*, another important transcriptional regulator of Th17 cell differentiation, rescued the increased generation of CCR6^{+} Th17 cells (Supplementary Fig. 3). Individual siRNAs against *Hif1a* also partially rescued the increased frequency of CCR6^{+}RORγt^{+} Th17 cells (Fig. 6A). Targeting either of these genes also reduced IL-17 production (Supplementary Fig. 3). As previously reported (31, 32), siRNAs targeting *Pten* promoted IL-17A production, but they did so without consistently affecting the generation of CCR6^{+}RORγt^{+} Th17 cells (Fig. 6A and Supplementary Fig. 3).

To further validate direct miRNA targeting of candidate target genes from the siRNA screen, we used 3′UTR dual luciferase reporter assays in primary mouse T cells. Although *Smad4* lacks a predicted miR-18 binding site, it had previously been suggested to be a miR-18 target (49). While we did detect de-repression of the annotated *Smad4* 3′UTR reporter in 17~92$^{\Delta/\Delta}$ CD4^{+} T cells (Fig. 6B), we could not significantly reverse that effect with any individual miRNA mimic (Fig. 6C). Based on RNA sequencing results ((50) and data not shown), we suspected that a longer *Smad4* transcript with an extended 3′UTR might be the functionally relevant target in this system. Quantitative RT-PCR confirmed that such a

transcript is indeed expressed in naïve $CD4^+$ T cells (Supplementary Fig. 4), and a *Smad4* 3′UTR extension segment luciferase reporter was inhibited by both miR-18a and miR-17 in transfected *Dgcr8*$^{\Delta/\Delta}$ $CD4^+$ T cells (Fig. 6D). The *Hif1a* 3′UTR reporter was also de-repressed in 17~92$^{\Delta/\Delta}$ $CD4^+$ T cells compared to 17~92$^{+/+}$ $CD4^+$ T cells (Fig. 6E). Importantly, the *Hif1a* 3′UTR was responsive to miR-18a as well as miR-17, establishing *Hif1a* as a novel miR-18 target (Fig. 6F). Finally, miR-18a repressed *Rora* 3′UTR reporter expression in 17~92$^{\Delta/\Delta}$ $CD4^+$ T cells, providing further evidence (34) that *Rora* is a direct target of miR-18a, even in the presence of residual miR-17 family activity (Fig. 6G). Biochemical evidence of Ago2 binding further supports direct miR-18a targeting of *Smad4*, *Hif1a* and *Rora* (51).

These data showed that miR-18a directly targets three transcription factors that are important inducers of the Th17 cell gene expression program. siRNA experiments also indicated that all three of these transcription factors could be limiting factors for Th17 cell differentiation, suggesting that regulation by miR-17~92 cluster miRNAs could impact their function. To further test this possibility, we generated 17~92$^{\Delta/\Delta}$ $CD4^+$ T cells that were also heterozygous for either the *Rora*^{sg} mutation (which encodes a nonfunctional truncated RORα protein) or a targeted conditional loss-of-function *Smad4* allele (*Smad4*$^{\Delta}$). $CD4^+$ T cells from both 17~92$^{\Delta/\Delta}$*Rora*$^{sg/+}$ (Fig. 6H) and 17~92$^{\Delta/\Delta}$*Smad4*$^{\Delta/+}$ (Fig. 6I) mice exhibited a decrease in the characteristic elevated frequency of 17~92$^{\Delta/\Delta}$ $CCR6^+ROR\gamma t^+$ cells to near miR-17~92$^{+/+}$ control levels, especially when cultured in Th17 conditions with higher doses of TGFβ. Thus, genetically limiting *Rora* or *Smad4* to one allele partially rescued the 17~92$^{\Delta/\Delta}$ phenotype. In summary, these data strongly suggest that *Smad4*, *Hif1a*, and *Rora* are all functionally relevant target genes of miR-18a.

Discussion

Here, we showed that miR-18a inhibits Th17 cell differentiation, and that this function stands in contrast to other members of the miR-17~92 cluster. Our experiments revealed that miR-18a is the most dynamically regulated miRNA of the miR-17~92 cluster in developing Th17 cells. Individually restoring each miRNA of the miR-17~92 cluster by transfection of 17~92$^{\Delta/\Delta}$ $CD4^+$ T cells with miRNA mimics revealed miR-18a's ability to inhibit Th17 cell differentiation, while other cluster members actually further enhanced Th17 cell differentiation. Importantly, these observations were further corroborated by *in vitro* and *in vivo* experiments utilizing $CD4^+$ T cells from miR-18a-deficient mice. CCR6 and RORγt expression were also increased in mouse and human $CD4^+$T cells transfected with miR-18 family-specific inhibitors. Mechanistically, we identified and validated three miR-18a target genes that encode transcription factors important for Th17 cell differentiation, including *Smad4*, a component of the TGFβ signaling pathway, *Hif1a*, an important target of miR-210 in its regulation of Th17 cell differentiation (18), and *Rora*, which we had previously shown to prevent subset-inappropriate gene expression in Tfh cells (34). The finding that miR-18a inhibits Th17 differentiation contrasts strikingly with previous work that described the miR-17~92 cluster's many roles as a positive regulator of $CD4^+$ T cell differentiation, including Th1 cells (35), Tfh cells (34, 38, 39) and Th2 cells (31). Overall, the present study illustrates how redundancy within families and clusters, coupled with signal-regulated

expression, enables miRNAs to confer robustness to T cell differentiation by targeting multiple genes in convergent pathways.

While Th1 and Th2 cell subsets were initially regarded as stable ‘lineages’, more recent work, especially on Th17 and Treg cells, has drawn attention to the plasticity and flexibility of Th cell subsets (1, 52). Th cell differentiation is driven by the balanced expression of key transcription factors that form a regulatory network in which small changes in gene expression determine cell fate decisions (52). One important layer of gene regulation that contributes to the control of these processes consists of evolutionary highly conserved miRNAs (21). For example, we and others have previously shown the importance of the miR-17~92 cluster for promoting robust Tfh cell differentiation (34, 38, 39). In addition, miR-17~92-deficient Tfh cells in appropriately upregulated a set of genes that are normally associated with Th17 cells, including *Ccr6*, *Il1r1*, *Il1r2*, the cytokine *Il22*, and the transcription factor *Rora*, the latter being a direct target of all four miRNA families represented in the miR-17~92 cluster (34). Thus, miR-17~92 emerges as a central regulator of Th cell plasticity, e.g. by preventing a Th17 program in differentiating Tfh cells (53).

Two previous reports implicated miR-17~92 miRNAs or related family members in the regulation of Th17 cell biology (32, 33). In one study, miR-17 and miR-19b were identified as responsible miR-17~92 miRNAs that promoted Th17-mediated inflammation (32). This is consistent with our finding that miR-17, miR-20a, and miR-19b mimics further enhanced CCR6 and IL-17A expression in $17{\sim}92^{\Delta/\Delta}$ Th17 cells. We extended these findings by showing that inhibition of the entire miR-17 family decreased IL-17A production. Multiple lines of evidence, including new siRNA experiments presented herein, indicate that *Pten* is an important miR-17~92 target gene that regulates IL-17 production (31, 32). Nevertheless, we did not observe a consistent decrease in IL-17 production in $17{\sim}92^{\Delta/\Delta}$ $CD4^+$ T cells *in vitro*, indicating the presence of counter-regulation of Th17 differentiation through other miR-17~92 target genes. This possibility was raised in a previous study in which decreased IL-17 production was observed in miR-17~92-deficient $CD4^+$ T cells using different Th17 culture conditions with additional polarizing cytokines (IL-1β and IL-23) and a longer culture period prior to analysis (32). Interestingly, the same study also showed an increase in *Rora* expression in miR-17~92-deficient $CD4^+$ T cells, consistent with our earlier work on Tfh cells (34) and data presented in the current study showing that *Rora* is a direct miR-18a target gene involved in Th17 cell differentiation. RORα and RORγt play redundant roles in inducing Th17 signature genes, including *Ccr6* (11). A second study showed that miR-20b can directly target *Stat3* and *Rorc*, further suggesting a complex balancing role for the miR-17 family in the regulation of IL-17 production (33). Our results extend these previous and other studies that focused on the varying roles of the miR-17~92 cluster in T cell biology and, importantly, identify a novel and distinct role for miR-18a as an inhibitor of Th17 cell differentiation.

The large impact of miR-18a in determining the net effect of miR-17~92 deficiency may be a product of the differential expression of individual miR-17~92 miRNAs and their related family members in differentiating Th17 cells. T cells strongly express the paralogous miR-106b~25 cluster, which contains two miR-17 family members and one miR-92 family member, and also retain weak but detectable expression of the miR-106a~363 cluster.

Activity sensors revealed that 17~92$^{\Delta/\Delta}$ CD4^{+} T cells almost completely lack miR-18 family activity, but retain a large fraction of the miR-17 and miR-92 family activity observed in wildtype CD4^{+} T cells, and a small residual amount of miR-19 family activity. These findings may explain why so many of the requirements for miR-17~92 in T cell biology have been mapped to miR-19 family function.

The importance of miR-18a function in Th17 cells may also relate to its particularly dynamic regulation during Th17 cell differentiation. *Mirc1* transcription is induced in activated T cells (54), but expression of the mature miR-17~92 cluster miRNAs is subject to differential regulation. Our data suggest that mature miR-92a induction may be limited by pre-processing of the primary miR-17~92 transcript in developing Th17 cells similarly as in differentiating ES cells (55). They also indicate further independent regulation of miR-18a processing or stability that maintains it at very low abundance in naïve T cells and allows it to be sharply upregulated during T cell activation (Fig. 1B and (46, 56)). miR-18a is also the most strongly upregulated miRNA in response to Myc-induced miR-17~92 transcription (57). Previous studies have indicated that miR-17, miR-19a, and miR-20a are also specifically regulated in lymphocytes during disease processes that they promote, including lymphomagenesis and allergic inflammation in asthma (30, 31). Further studies are needed to dissect the intricate regulation of miR-17~92 and its paralogs, and the relationships between regulated expression and the biological functions of each mature miRNA. Complete deficiency in miR-17, miR-18, and miR-19 could be studied in mice lacking all three paralogous clusters (39), and each miRNA in the miR-17~92 cluster could be further interrogated using recently reported miR-17~92 allelic series mutant mice (42), which include the miR-18$^{\Delta/\Delta}$ mice that we used in this study.

The distinct regulation and functions of miR-18a and miR-17 illustrate how a cluster of miRNAs can evolve to exert nuanced regulation of gene expression and cell behavior. Phylogenetic comparison suggests that miR-18a was created by a duplication of miR-17 that shifted the miRNA seed sequence by a single nucleotide. As such, miR-18a and miR-17 share many target binding sites, such as in the *Smad4* 3′UTR extension. Yet these two miRNAs have diverged and acquired independent targets (42), differential regulation of processing and/or stability during T cell activation, and different degrees of redundancy with miRNAs in other clusters. Together, these features allow T cells to translate environmental signals into complex regulation of immune responses through closely related miRNAs within a single miRNA cluster. In future studies, it will be interesting to investigate the upstream mechanisms that regulate the induction of miR-17~92 expression and the differential expression and processing of the individual cluster miRNAs. Given their clear functional differences in regards to regulating Th17 differentiation, this is particularly the case for the closely related miRNAs miR-18a and miR-17.

Our experiments revealed a cell-intrinsic role for miR-18 in Th17 cell differentiation *in vitro* and corresponding changes in lung inflammation in miR-18$^{\Delta/\Delta}$ mice *in vivo*. In future studies, it will be important to examine the intrinsic limiting role of miR-18 in Th17 cells *in vivo* and to explore the interesting possibility that miR-18 may further influence inflammatory responses through independent effects in other cell types. One advantage of using CD4^{+} T cells from miR-18$^{\Delta/\Delta}$ mice for these studies is that we did not observe any

differences in their proliferative or survival capacities. This is in clear contrast to miR-17~92-deficient $CD4^+$ T cells, which show impaired proliferation, expansion and survival, thus limiting their use for *in vivo* models in which these altered processes clearly influence the pathophysiological outcomes of the experimental system. In summary, our detailed functional analyses of miR-18a in activated $CD4^+$ T cells *in vitro* and *in vivo* highlight the distinct negative impact of this miRNA on Th17 cell differentiation, which is in clear contrast to the function of the other miR-17~92 cluster members. These insights might provide the basis for the development of therapeutic approaches that strengthen the expression of this miRNA or inhibit its target genes.

Supplementary Material

Refer to Web version on PubMed Central for supplementary material.

Acknowledgments

We would like to thank Sana Patel and Jeanmarie Gonzales for expert technical assistance, and Andrea Ventura for providing miR-18a$^{\Delta/\Delta}$ mice.

References

1. Sallusto F. Heterogeneity of Human CD4(+) T Cells Against Microbes. Annu Rev Immunol. 2016; 34:317–334. [PubMed: 27168241]
2. Korn T, Bettelli E, Oukka M, Kuchroo VK. IL-17 and Th17 Cells. Annu Rev Immunol. 2009; 27:485–517. [PubMed: 19132915]
3. Gaffen SL, Jain R, Garg AV, Cua DJ. The IL-23-IL-17 immune axis: from mechanisms to therapeutic testing. Nat Rev Immunol. 2014; 14:585–600. [PubMed: 25145755]
4. Weaver CT, Elson CO, Fouser LA, Kolls JK. The Th17 pathway and inflammatory diseases of the intestines, lungs, and skin. Annual review of pathology. 2013; 8:477–512.
5. Pappu R, Rutz S, Ouyang W. Regulation of epithelial immunity by IL-17 family cytokines. Trends Immunol. 2012; 33:343–349. [PubMed: 22476048]
6. Choy DF, Hart KM, Borthwick LA, Shikotra A, Nagarkar DR, Siddiqui S, Jia G, Ohri CM, Doran E, Vannella KM, Butler CA, Hargadon B, Sciurba JC, Gieseck RL, Thompson RW, White S, Abbas AR, Jackman J, Wu LC, Egen JG, Heaney LG, Ramalingam TR, Arron JR, Wynn TA, Bradding P. TH2 and TH17 inflammatory pathways are reciprocally regulated in asthma. Science translational medicine. 2015; 7:301ra129.
7. Newcomb DC, Boswell MG, Huckabee MM, Goleniewska K, Dulek DE, Reiss S, Lukacs NW, Kolls JK, Peebles RS Jr. IL-13 regulates Th17 secretion of IL-17A in an IL-10-dependent manner. J Immunol. 2012; 188:1027–1035. [PubMed: 22210911]
8. Veldhoen M, Hocking RJ, Atkins CJ, Locksley RM, Stockinger B. TGFbeta in the context of an inflammatory cytokine milieu supports de novo differentiation of IL-17-producing T cells. Immunity. 2006; 24:179–189. [PubMed: 16473830]
9. Mangan PR, Harrington LE, O'Quinn DB, Helms WS, Bullard DC, Elson CO, Hatton RD, Wahl SM, Schoeb TR, Weaver CT. Transforming growth factor-beta induces development of the T(H)17 lineage. Nature. 2006; 441:231–234. [PubMed: 16648837]
10. Bettelli E, Carrier Y, Gao W, Korn T, Strom TB, Oukka M, Weiner HL, Kuchroo VK. Reciprocal developmental pathways for the generation of pathogenic effector TH17 and regulatory T cells. Nature. 2006; 441:235–238. [PubMed: 16648838]
11. Yang XO, Pappu BP, Nurieva R, Akimzhanov A, Kang HS, Chung Y, Ma L, Shah B, Panopoulos AD, Schluns KS, Watowich SS, Tian Q, Jetten AM, Dong C. T helper 17 lineage differentiation is programmed by orphan nuclear receptors ROR alpha and ROR gamma. Immunity. 2008; 28:29–39. [PubMed: 18164222]

12. Yamazaki T, Yang XO, Chung Y, Fukunaga A, Nurieva R, Pappu B, Martin-Orozco N, Kang HS, Ma L, Panopoulos AD, Craig S, Watowich SS, Jetten AM, Tian Q, Dong C. CCR6 regulates the migration of inflammatory and regulatory T cells. J Immunol. 2008; 181:8391–8401. [PubMed: 19050256]
13. Reboldi A, Coisne C, Baumjohann D, Benvenuto F, Bottinelli D, Lira S, Uccelli A, Lanzavecchia A, Engelhardt B, Sallusto F. C-C chemokine receptor 6-regulated entry of TH-17 cells into the CNS through the choroid plexus is required for the initiation of EAE. Nat Immunol. 2009; 10:514–523. [PubMed: 19305396]
14. Acosta-Rodriguez EV, Rivino L, Geginat J, Jarrossay D, Gattorno M, Lanzavecchia A, Sallusto F, Napolitani G. Surface phenotype and antigenic specificity of human interleukin 17-producing T helper memory cells. Nat Immunol. 2007; 8:639–646. [PubMed: 17486092]
15. Annunziato F, Cosmi L, Santarlasci V, Maggi L, Liotta F, Mazzinghi B, Parente E, Fili L, Ferri S, Frosali F, Giudici F, Romagnani P, Parronchi P, Tonelli F, Maggi E, Romagnani S. Phenotypic and functional features of human Th17 cells. J Exp Med. 2007; 204:1849–1861. [PubMed: 17635957]
16. Ciofani M, Madar A, Galan C, Sellars M, Mace K, Pauli F, Agarwal A, Huang W, Parkurst CN, Muratet M, Newberry KM, Meadows S, Greenfield A, Yang Y, Jain P, Kirigin FK, Birchmeier C, Wagner EF, Murphy KM, Myers RM, Bonneau R, Littman DR. A validated regulatory network for Th17 cell specification. Cell. 2012; 151:289–303. [PubMed: 23021777]
17. Yosef N, Shalek AK, Gaublomme JT, Jin H, Lee Y, Awasthi A, Wu C, Karwacz K, Xiao S, Jorgolli M, Gennert D, Satija R, Shakya A, Lu DY, Trombetta JJ, Pillai MR, Ratcliffe PJ, Coleman ML, Bix M, Tantin D, Park H, Kuchroo VK, Regev A. Dynamic regulatory network controlling TH17 cell differentiation. Nature. 2013; 496:461–468. [PubMed: 23467089]
18. Wang H, Flach H, Onizawa M, Wei L, McManus MT, Weiss A. Negative regulation of Hif1a expression and TH17 differentiation by the hypoxia-regulated microRNA miR-210. Nat Immunol. 2014; 15:393–401. [PubMed: 24608041]
19. Shi LZ, Wang R, Huang G, Vogel P, Neale G, Green DR, Chi H. HIF1alpha-dependent glycolytic pathway orchestrates a metabolic checkpoint for the differentiation of TH17 and Treg cells. J Exp Med. 2011; 208:1367–1376. [PubMed: 21708926]
20. Dang EV, Barbi J, Yang HY, Jinasena D, Yu H, Zheng Y, Bordman Z, Fu J, Kim Y, Yen HR, Luo W, Zeller K, Shimoda L, Topalian SL, Semenza GL, Dang CV, Pardoll DM, Pan F. Control of T(H)17/T(reg) balance by hypoxia-inducible factor 1. Cell. 2011; 146:772–784. [PubMed: 21871655]
21. Baumjohann D, Ansel KM. MicroRNA-mediated regulation of T helper cell differentiation and plasticity. Nat Rev Immunol. 2013; 13:666–678. [PubMed: 23907446]
22. Cobb BS, Hertweck A, Smith J, O'Connor E, Graf D, Cook T, Smale ST, Sakaguchi S, Livesey FJ, Fisher AG, Merkenschlager M. A role for Dicer in immune regulation. J Exp Med. 2006; 203:2519–2527. [PubMed: 17060477]
23. Escobar TM, Kanellopoulou C, Kugler DG, Kilaru G, Nguyen CK, Nagarajan V, Bhairavabhotla RK, Northrup D, Zahr R, Burr P, Liu X, Zhao K, Sher A, Jankovic D, Zhu J, Muljo SA. miR-155 activates cytokine gene expression in Th17 cells by regulating the DNA-binding protein Jarid2 to relieve polycomb-mediated repression. Immunity. 2014; 40:865–879. [PubMed: 24856900]
24. Du C, Liu C, Kang J, Zhao G, Ye Z, Huang S, Li Z, Wu Z, Pei G. MicroRNA miR-326 regulates TH-17 differentiation and is associated with the pathogenesis of multiple sclerosis. Nat Immunol. 2009; 10:1252–1259. [PubMed: 19838199]
25. O'Connell RM, Kahn D, Gibson WS, Round JL, Scholz RL, Chaudhuri AA, Kahn ME, Rao DS, Baltimore D. MicroRNA-155 promotes autoimmune inflammation by enhancing inflammatory T cell development. Immunity. 2010; 33:607–619. [PubMed: 20888269]
26. Zhu S, Pan W, Song X, Liu Y, Shao X, Tang Y, Liang D, He D, Wang H, Liu W, Shi Y, Harley JB, Shen N, Qian Y. The microRNA miR-23b suppresses IL-17-associated autoimmune inflammation by targeting TAB2, TAB3 and IKK-alpha. Nat Med. 2012; 18:1077–1086. [PubMed: 22660635]
27. Mycko MP, Cichalewska M, Machlanska A, Cwiklinska H, Mariasiewicz M, Selmaj KW. MicroRNA-301a regulation of a T-helper 17 immune response controls autoimmune demyelination. Proc Natl Acad Sci U S A. 2012; 109:E1248–1257. [PubMed: 22517757]

28. Hu R, Huffaker TB, Kagele DA, Runtsch MC, Bake E, Chaudhuri AA, Round JL, O'Connell RM. MicroRNA-155 confers encephalogenic potential to Th17 cells by promoting effector gene expression. J Immunol. 2013; 190:5972–5980. [PubMed: 23686497]
29. Murugaiyan G, Beynon V, Mittal A, Joller N, Weiner HL. Silencing microRNA-155 ameliorates experimental autoimmune encephalomyelitis. J Immunol. 2011; 187:2213–2221. [PubMed: 21788439]
30. Olive V, Li Q, He L. mir-17-92: a polycistronic oncomir with pleiotropic functions. Immunol Rev. 2013; 253:158–166. [PubMed: 23550645]
31. Simpson LJ, Patel S, Bhakta NR, Choy DF, Brightbill HD, Ren X, Wang Y, Pua HH, Baumjohann D, Montoya MM, Panduro M, Remedios KA, Huang X, Fahy JV, Arron JR, Woodruff PG, Ansel KM. A microRNA upregulated in asthma airway T cells promotes TH2 cytokine production. Nat Immunol. 2014; 15:1162–1170. [PubMed: 25362490]
32. Liu SQ, Jiang S, Li C, Zhang B, Li QJ. miR-17-92 cluster targets phosphatase and tensin homology and Ikaros Family Zinc Finger 4 to promote TH17-mediated inflammation. J Biol Chem. 2014; 289:12446–12456. [PubMed: 24644282]
33. Zhu E, Wang X, Zheng B, Wang Q, Hao J, Chen S, Zhao Q, Zhao L, Wu Z, Yin Z. miR-20b Suppresses Th17 Differentiation and the Pathogenesis of Experimental Autoimmune Encephalomyelitis by Targeting RORgammat and STAT3. J Immunol. 2014; 192:5599–5609. [PubMed: 24842756]
34. Baumjohann D, Kageyama R, Clingan JM, Morar MM, Patel S, de Kouchkovsky D, Bannard O, Bluestone JA, Matloubian M, Ansel KM, Jeker LT. The microRNA cluster miR-17 approximately 92 promotes TFH cell differentiation and represses subset-inappropriate gene expression. Nat Immunol. 2013; 14:840–848. [PubMed: 23812098]
35. Jiang S, Li C, Olive V, Lykken E, Feng F, Sevilla J, Wan Y, He L, Li QJ. Molecular dissection of the miR-17-92 cluster's critical dual roles in promoting Th1 responses and preventing inducible Treg differentiation. Blood. 2011; 118:5487–5497. [PubMed: 21972292]
36. de Kouchkovsky D, Esensten JH, Rosenthal WL, Morar MM, Bluestone JA, Jeker LT. microRNA-17-92 regulates IL-10 production by regulatory T cells and control of experimental autoimmune encephalomyelitis. J Immunol. 2013; 191:1594–1605. [PubMed: 23858035]
37. Yang HY, Barbi J, Wu CY, Zheng Y, Vignali PD, Wu X, Tao JH, Park BV, Bandara S, Novack L, Ni X, Yang X, Chang KY, Wu RC, Zhang J, Yang CW, Pardoll DM, Li H, Pan F. MicroRNA-17 Modulates Regulatory T Cell Function by Targeting Co-regulators of the Foxp3 Transcription Factor. Immunity. 2016; 45:83–93. [PubMed: 27438767]
38. Wu T, Wieland A, Lee J, Hale JS, Han JH, Xu X, Ahmed R. Cutting Edge: miR-17-92 Is Required for Both CD4 Th1 and T Follicular Helper Cell Responses during Viral Infection. J Immunol. 2015
39. Kang SG, Liu WH, Lu P, Jin HY, Lim HW, Shepherd J, Fremgen D, Verdin E, Oldstone MB, Qi H, Teijaro JR, Xiao C. MicroRNAs of the miR-17 approximately 92 family are critical regulators of TFH differentiation. Nat Immunol. 2013; 14:849–857. [PubMed: 23812097]
40. Xiao C, Srinivasan L, Calado DP, Patterson HC, Zhang B, Wang J, Henderson JM, Kutok JL, Rajewsky K. Lymphoproliferative disease and autoimmunity in mice with increased miR-17-92 expression in lymphocytes. Nat Immunol. 2008; 9:405–414. [PubMed: 18327259]
41. Steiner DF, Thomas MF, Hu JK, Yang Z, Babiarz JE, Allen CD, Matloubian M, Blelloch R, Ansel KM. MicroRNA-29 Regulates T-Box Transcription Factors and Interferon-gamma Production in Helper T Cells. Immunity. 2011; 35:169–181. [PubMed: 21820330]
42. Han YC, Vidigal JA, Mu P, Yao E, Singh I, Gonzalez AJ, Concepcion CP, Bonetti C, Ogrodowski P, Carver B, Selleri L, Betel D, Leslie C, Ventura A. An allelic series of miR-17 approximately 92-mutant mice uncovers functional specialization and cooperation among members of a microRNA polycistron. Nat Genet. 2015; 47:766–775. [PubMed: 26029871]
43. Rao PK, Toyama Y, Chiang HR, Gupta S, Bauer M, Medvid R, Reinhardt F, Liao R, Krieger M, Jaenisch R, Lodish HF, Blelloch R. Loss of cardiac microRNA-mediated regulation leads to dilated cardiomyopathy and heart failure. Circ Res. 2009; 105:585–594. [PubMed: 19679836]
44. Baumjohann D, Ansel KM. Tracking early T follicular helper cell differentiation in vivo. Methods Mol Biol. 2015; 1291:27–38. [PubMed: 25836299]

45. Kozomara A, Griffiths-Jones S. miRBase: annotating high confidence microRNAs using deep sequencing data. Nucleic Acids Res. 2014; 42:D68–73. [PubMed: 24275495]

46. Kuchen S, Resch W, Yamane A, Kuo N, Li Z, Chakraborty T, Wei L, Laurence A, Yasuda T, Peng S, Hu-Li J, Lu K, Dubois W, Kitamura Y, Charles N, Sun HW, Muljo S, Schwartzberg PL, Paul WE, O'Shea J, Rajewsky K, Casellas R. Regulation of microRNA expression and abundance during lymphopoiesis. Immunity. 2010; 32:828–839. [PubMed: 20605486]

47. Cosmi L, Liotta F, Maggi E, Romagnani S, Annunziato F. Th17 cells: new players in asthma pathogenesis. Allergy. 2011; 66:989–998. [PubMed: 21375540]

48. Hsu SD, Lin FM, Wu WY, Liang C, Huang WC, Chan WL, Tsai WT, Chen GZ, Lee CJ, Chiu CM, Chien CH, Wu MC, Huang CY, Tsou AP, Huang HD. miRTarBase: a database curates experimentally validated microRNA-target interactions. Nucleic Acids Res. 2011; 39:D163–169. [PubMed: 21071411]

49. Li L, Shi JY, Zhu GQ, Shi B. MiR-17-92 cluster regulates cell proliferation and collagen synthesis by targeting TGFB pathway in mouse palatal mesenchymal cells. J Cell Biochem. 2012; 113:1235–1244. [PubMed: 22095742]

50. Agarwal V, Bell GW, Nam JW, Bartel DP. Predicting effective microRNA target sites in mammalian mRNAs. Elife. 2015; 4

51. Loeb GB, Khan AA, Canner D, Hiatt JB, Shendure J, Darnell RB, Leslie CS, Rudensky AY. Transcriptome-wide miR-155 Binding Map Reveals Widespread Noncanonical MicroRNA Targeting. Molecular cell. 2012

52. O'Shea JJ, Paul WE. Mechanisms underlying lineage commitment and plasticity of helper CD4+ T cells. Science. 2010; 327:1098–1102. [PubMed: 20185720]

53. Maul J, Baumjohann D. Emerging Roles for MicroRNAs in T Follicular Helper Cell Differentiation. Trends Immunol. 2016; 37:297–309. [PubMed: 27068008]

54. Bronevetsky Y, Villarino AV, Eisley CJ, Barbeau R, Barczak AJ, Heinz GA, Kremmer E, Heissmeyer V, McManus MT, Erle DJ, Rao A, Ansel KM. T cell activation induces proteasomal degradation of Argonaute and rapid remodeling of the microRNA repertoire. J Exp Med. 2013; 210:417–432. [PubMed: 23382546]

55. Du P, Wang L, Sliz P, Gregory RI. A Biogenesis Step Upstream of Microprocessor Controls miR-17 approximately 92 Expression. Cell. 2015; 162:885–899. [PubMed: 26255770]

56. Barski A, Jothi R, Cuddapah S, Cui K, Roh TY, Schones DE, Zhao K. Chromatin poises miRNA- and protein-coding genes for expression. Genome Res. 2009; 19:1742–1751. [PubMed: 19713549]

57. O'Donnell KA, Wentzel EA, Zeller KI, Dang CV, Mendell JT. c-Myc-regulated microRNAs modulate E2F1 expression. Nature. 2005; 435:839–843. [PubMed: 15944709]

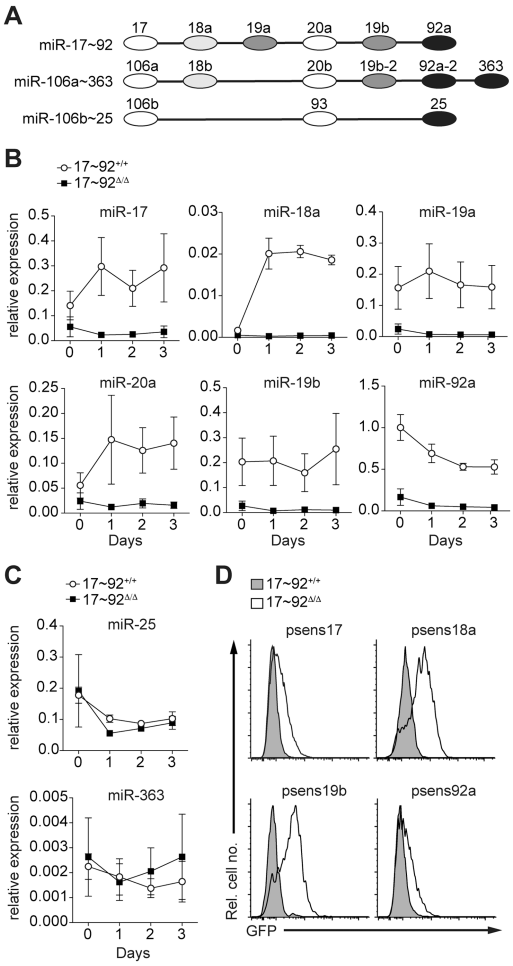

Figure 1. miR-18a is active and dynamically regulated during Th17 cell differentiation

(**A**) Schematic of miRNAs within the miR-17~92 cluster and its paralogous miRNA gene clusters miR-106a~363 and miR-106b~25. Individual miRNA families represented in the three clusters are color-coded. (**B, C**) Naive control ($17{\sim}92^{+/+}$; circles) and miR-17~92-deficient ($17{\sim}92^{\Delta/\Delta}$; squares) $CD4^+$ T cells were cultured *in vitro* under Th17-polarizing conditions. Cells were harvested at the indicated time points and quantitative real-time PCR was performed to determine expression levels of individual miRNAs of the miR-17~92 cluster (**B**) or representative miRNAs from the paralogous miRNA gene clusters miR-106b~25 and miR-106a~363 (**C**); expression was normalized to 5.8S rRNA in each sample. (**D**) $17{\sim}92^{+/+}$ and $17{\sim}92^{\Delta/\Delta}$ $CD4^+$ T cells were transduced with retroviral sensors expressing EGFP together with 4 perfectly complementary binding sites for miR-17 (psens17), miR-18a (psens18a), miR-19b (psens19b) or miR-92a (psens92a) in the 3′UTR and analyzed by flow cytometry. Data are pooled from three independent experiments, each with one mouse per genotype (**B, C**; error bars represent s.e.m.) or are representative of four independent experiments, each with one mouse per genotype (**D**).

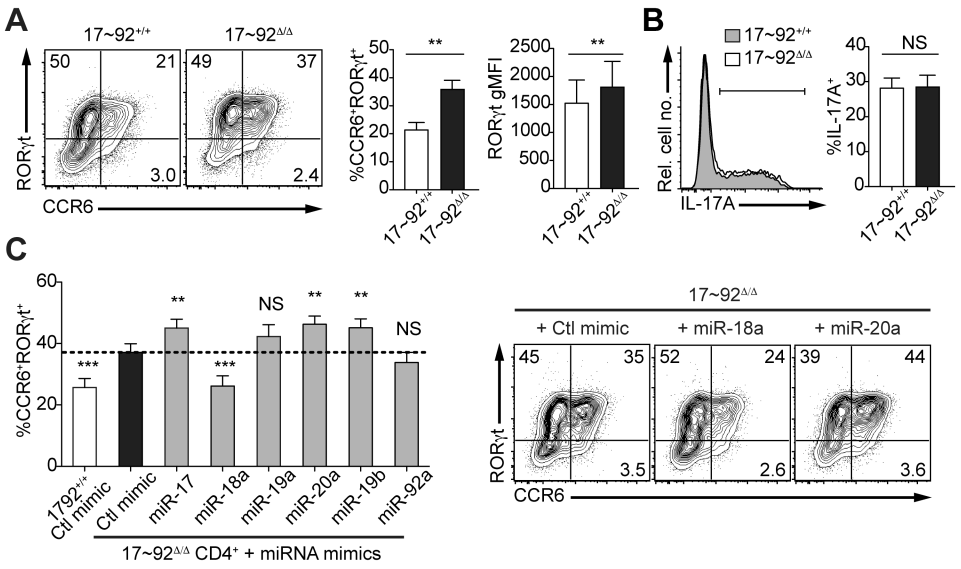

Figure 2. miR-18a inhibits Th17 cell differentiation

Naive 17~92$^{+/+}$ and 17~92$^{\Delta/\Delta}$ CD4^{+} T cells were cultured *in vitro* under Th17 conditions (TGFβ+IL-6) and analyzed on day 3.5 for Th17 marker expression by flow cytometry. (**A**) Representative contour plots show surface CCR6 and intracellular RORγt co-staining of live singlet CD4^{+} T cells. Frequencies of CCR6^{+} and CCR6^{+}RORγt^{+} cells as well as the RORγt geometric mean fluorescence intensity (gMFI) are quantified in the bar graphs. (**B**) IL-17A production after restimulation with PMA/ionomycin is shown in a representative histogram and the frequency of IL-17A^{+} cells is quantified in the bar graph. (**C**) Naive 17~92$^{+/+}$ and 17~92$^{\Delta/\Delta}$ CD4^{+} T cells were cultured under Th17-polarizing conditions and transfected on day 2 with control miRNA mimics (Ctl mimic) or miRNA mimics of the individual miR-17~92 cluster members. Cells were analyzed on day 3.5 for Th17 marker expression by flow cytometry. The frequencies of CCR6^{+}RORγt^{+} cells among CD4^{+} T cells are shown in the bar graph; representative contour plots display surface CCR6 expression and intracellular RORγt co-staining of CD4^{+} T cells. Numbers in quadrants indicate percent CCR6 and/or RORγt-positive live singlet cells. **P<0.01 and ***P<0.001 (two-tailed paired *t*-test with pre-assigned littermate pairs (**A, B**) or one-way ANOVA with Dunnett's multiple comparison post-test comparing all columns to control miRNA mimic-transfected 17~92$^{\Delta/\Delta}$ CD4^{+} T cells (**C**)). Data are pooled from five (**C**), or six to eight (**A, B**) independent experiments, each with one to two mice per genotype (mean and s.e.m.; **A**-**C**).

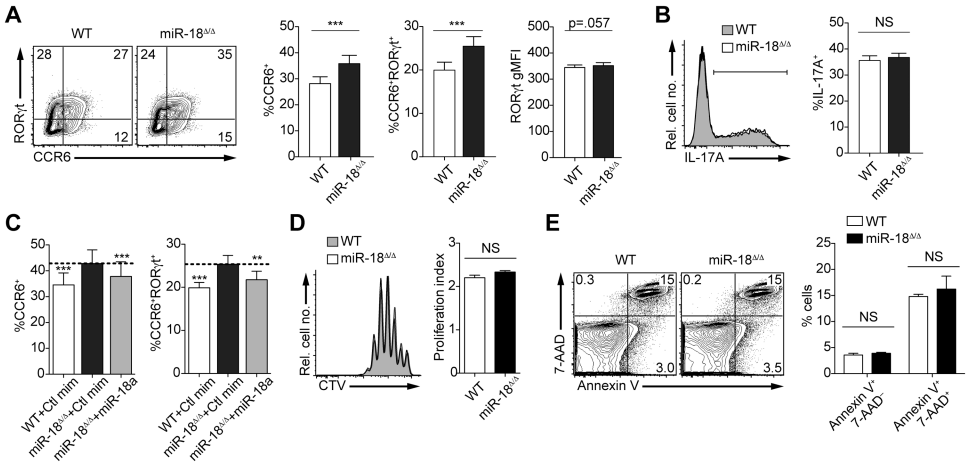

Figure 3. Genetic ablation of miR-18a alone increases the frequency of CCR6$^+$ and CCR6$^+$RORγt$^+$ CD4$^+$ T cells

Naive wildtype (WT) and miR-18$^{\Delta/\Delta}$ CD4$^+$ T cells were cultured *in vitro* under Th17 conditions (TGFβ+IL-6) and analyzed on day 3.5 for Th17 marker expression by flow cytometry. (**A**) Representative contour plots show surface CCR6 and intracellular RORγt co-staining of live singlet CD4$^+$ T cells. Frequencies of CCR6$^+$ and CCR6$^+$RORγt$^+$ cells as well as the RORγt gMFI are quantified in the bar graphs. (**B**) IL-17A production after restimulation with PMA/ionomycin is shown in a representative histogram and the frequency of IL-17A$^+$ cells is quantified in the bar graph. (**C**) Naive WT and miR-18$^{\Delta/\Delta}$ CD4$^+$ T cells were cultured under Th17-polarizing conditions and transfected on day 2 with control miRNA mimics (Ctlmim) or miR-18a mimics. Cells were analyzed by flow cytometry on day 3.5. The frequencies of CCR6$^+$ and CCR6$^+$RORγt$^+$ cells are quantified in the bar graphs. (**D**) Representative histograms show CellTrace Violet (CTV)-labeled cells assessed on day 3.5 of culture. Proliferation indices are quantified in the bar graph. (**E**) Frequencies of early apoptotic (Annexin V$^+$ 7-AAD$^-$) and late apoptotic/dead cells (Annexin V$^+$ 7-AAD$^+$) among WT and miR-18$^{\Delta/\Delta}$ CD4$^+$ T cells were assessed by flow cytometry on day 3.5 of Th17 culture. **P<0.01 and ***P<0.001 (two-tailed paired *t*-test with pre-assigned littermate pairs (**A, B, D, E**) or one-way ANOVA with Dunnett's multiple comparison post-test comparing all columns to control miRNA mimic-transfected miR-18$^{\Delta/\Delta}$ CD4$^+$ T cells (**C**)). Data are pooled from two independent experiments, each with three mice per genotype (**A, B, C**) or are representative of two independent experiments with three mice per group (**D, E**). Error bars represent s.e.m.

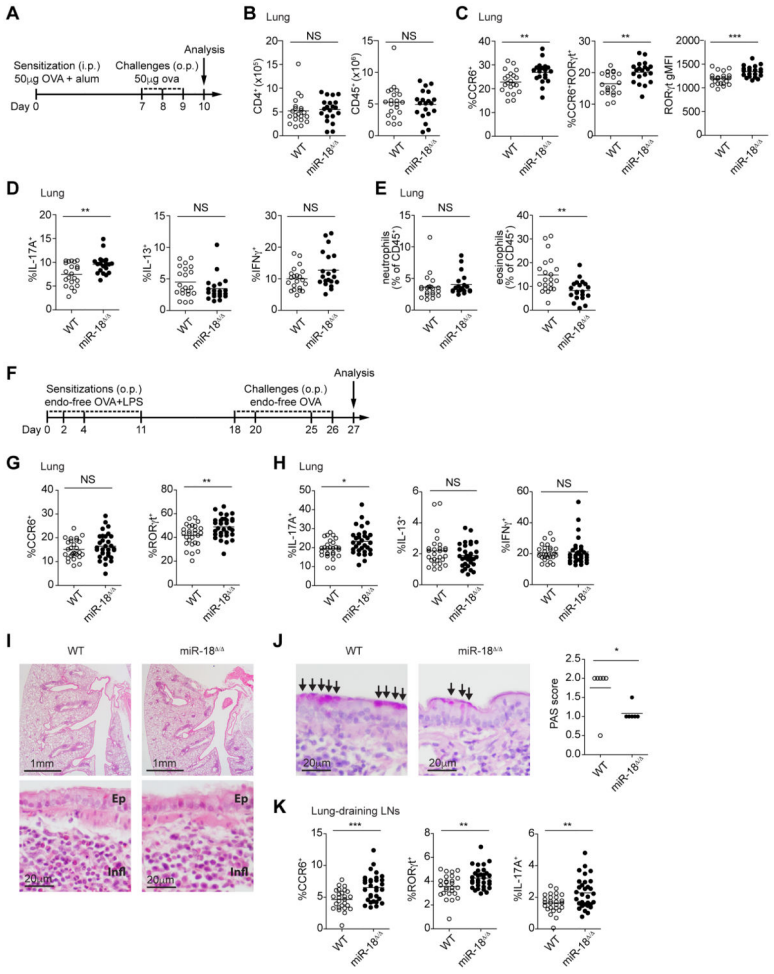

Figure 4. miR-18a deficiency increases lung Th17 cell frequencies in airway inflammation models

(**A**) Schematic of the 10-day *in vivo* airway hypersensitivity model with intraperitoneal (i.p.) OVA+alum sensitization on day 0, followed by three consecutive daily challenges with OVA oropharyngeally (o.p.) on days 7, 8, and 9. On day 10, cells from the lungs of WT and miR-18$^{\Delta/\Delta}$ mice were harvested and analyzed by flow cytometry. (**B**) Total CD4^{+} T cell and total CD45^{+} leukocyte numbers per lung. (**C**) Frequencies of CCR6^{+} and CCR6^{+}RORγt^{+} cells; intracellular RORγt expression levels as determined by gMFI. (**D**) Frequencies of IL-17A, IL-13 or IFNγ-producing cells among CD4^{+} T cells after restimulation with PMA/ionomycin. (**E**) Frequencies of inflammatory cells in the lungs, including eosinophils (CD11b^{+}SiglecF^{+}) and neutrophils (CD11b^{+}Ly6G^{+}). (**F**) Schematic of the 27-day *in vivo* airway hypersensitivity model with OVA+LPS sensitizations on days 0, 2, 4, and 11 by oropharyngeal instillation (o.p.), followed by OVA challenge on days 18, 20, 25, and 26. On day 27, cells from the lungs of WT and miR-18$^{\Delta/\Delta}$ mice were harvested and analyzed by flow cytometry. (**G**) Frequency of CCR6^{+} and RORγt^{+} cells among CD4^{+} T cells.(**H**) Frequency of IL-17A, IL-13, andIFNγ-producing cells among CD4^{+} T cells after restimulation with PMA/ionomycin. (**I**) Hematoxylin and eosin stainings of lungs derived from challenged WT and miR-18$^{\Delta/\Delta}$ mice. Two different magnifications are shown. Bronchiole epithelium (Ep) and mixed local inflammation (Infl) are marked for orientation

in high power fields. (**J**) Periodic acid-Schiff (PAS) staining highlighting goblet cell metaplasia of the respiratory epithelium (arrows). Histological scores of PAS staining quantifying mucus-secreting cells are quantified in the bar graph. (**K**) Lung-draining lymph nodes were analyzed by flow cytometry for the frequency of $CCR6^+$ and $ROR\gamma t^+$ cells as well as the frequency of IL-17A among $CD4^+$ T cells after restimulation with PMA/ionomycin. *P<0.05, **P<0.01 and ***P<0.001 (two-tailed unpaired *t*-test with pre-assigned littermate pairs). Data are pooled from three independent experiments, each with three to nine mice per genotype (n=21 mice total per genotype; **A-E**) or each with seven to twelve mice per genotype (n=26 to 31 mice total per genotype; **F-H, J, K**). Data in I is a representative experiment with six mice per genotype.

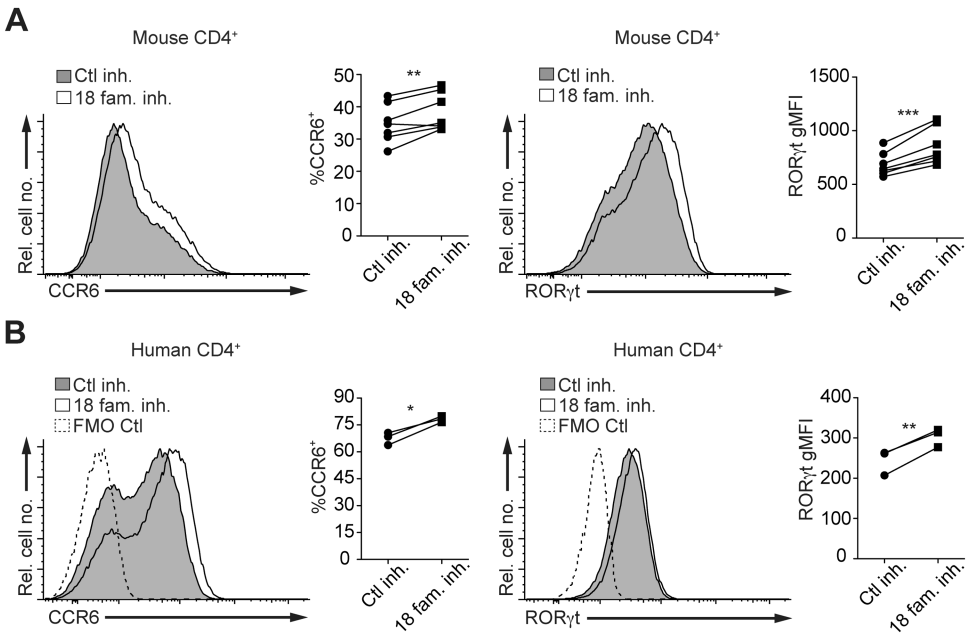

Figure 5. Inhibition of the miR-18 family increases mouse and human Th17 cell differentiation

(**A**) Murine WT CD4$^+$ T cells polarized under Th17 conditions *in vitro* and transfected with either control inhibitor (Ctl inh.) or miR-18 family inhibitor (18 fam. inh.) on day 2. Cells were analyzed by flow cytometry on day 3.5 of culture. Histograms show representative stainings of surface CCR6 and intracellular RORγt expression. Frequencies of CCR6$^+$ cells as well as RORγt gMFI are quantified in the dot plots. (**B**) CD4$^+$ T cells isolated from human cord blood were polarized under Th17 conditions *in vitro* and transfected with control inhibitor (Ctl inh.) or miR-18 family inhibitor (18 fam. inh.) on day 2. Cells were analyzed by flow cytometry on day 3.5 of culture. Histograms show representative stainings of surface CCR6 and intracellular RORγt expression. Frequencies of CCR6$^+$ cells as well as RORγt gMFI are quantified in the dot plots. Dashed lines represent background staining in the CCR6 or RORγt-detecting channels (fluorescence-minus-one (FMO) controls). Circles (Ctl inh.) and squares (18 fam. inh.) in the dot plots represent the mean of two to three individual transfections for each inhibitor (**A, B**); lines connect individual WT mice (**A**) or individual cord blood donors (**B**) that received respective inhibitors. *P<0.05, **P<0.01 and ***P<0.001 (two-tailed paired *t*-test). Data are pooled from three independent experiments with two to three mice per experiment (n=7) (**A**) or from one experiment with three different donor samples (n=3) (**B**).

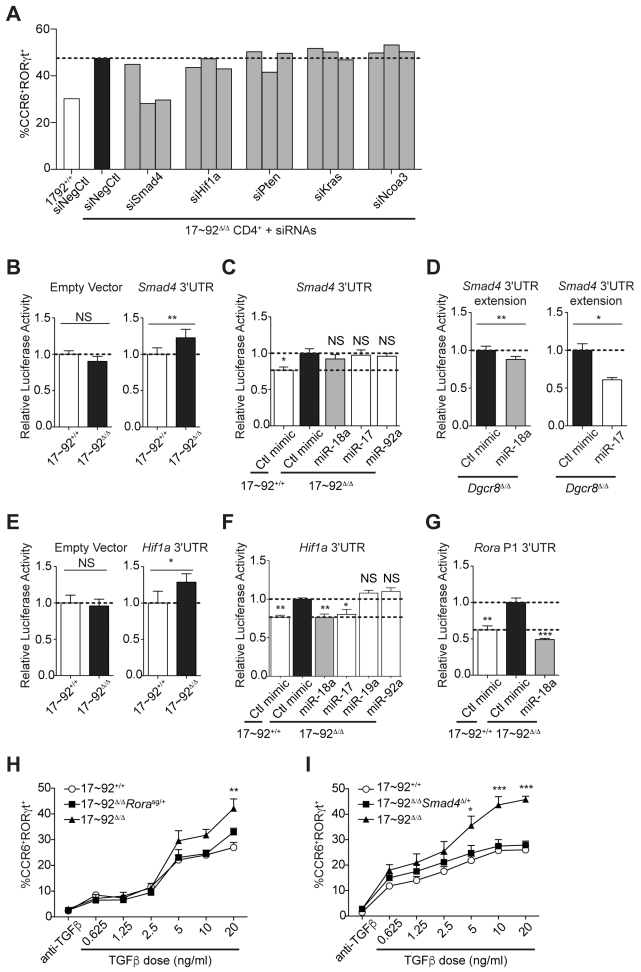

Figure 6. *Smad4*, *Hif1a,* and *Rora* are functionally relevant target genes of miR-18a

(**A**) Naive 17~92$^{+/+}$ and 17~92$^{\Delta/\Delta}$ CD4^{+} T cells were cultured under Th17-polarizing conditions and transfected with an siRNA non-targeting control (siNegCtl) or three individual siRNAs against each of five different candidate genes. Bars quantify the frequency of CCR6^{+}RORγt^{+} cells among live CD4^{+} singlet cells. Dashed line indicates the level of negative-control siRNA-transfected 17~92$^{\Delta/\Delta}$ CD4^{+} cells. (**B**) Renilla luciferase activity in 17~92$^{+/+}$ control and 17~92$^{\Delta/\Delta}$ CD4^{+} T cells transfected with empty vector or with dual luciferase reporters for *Smad4* 3′ untranslated (3′UTR) regions assessed 24 h after transfection; results were normalized to firefly luciferase activity and are presented relative to those of transfected 17~92$^{+/+}$ control CD4^{+} T cells. (**C**) Renilla luciferase activity in primary 17~92$^{+/+}$ control and 17~92$^{\Delta/\Delta}$ CD4+ T cells co-transfected with *Smad4* 3′UTR luciferase reporters and individual miR-17~92 miRNA mimics or Ctl mimic, assessed 24 h after transfection; results were normalized to firefly luciferase activity and are presented relative to those of control miRNA mimic-transfected 17~92$^{\Delta/\Delta}$ CD4^{+} T cells. (**D**) Renilla luciferase activity in global miRNA-deficient *Dgcr8*$^{\Delta/\Delta}$ CD4^{+} T cells co-transfected with the *Smad4* 3′UTR extension luciferase reporter and either control miRNA mimic (Ctl mimic) or miR-18a mimic (left) or with miR-17 mimic (right), assessed 24 h after transfection; results were normalized to firefly luciferase activity and are presented relative to those of control

miRNA mimic-transfected *Dgcr8*$^{\Delta/\Delta}$ CD4^{+} T cells. (**E**) Renilla luciferase activity of 17~92$^{+/+}$ control and 17~92$^{\Delta/\Delta}$ CD4^{+} T cells transfected with empty vector or with dual luciferase reporters for *Hif1a* 3′UTR regions as described in B. (**F**) Renilla luciferase activity in primary 17~92$^{+/+}$ control and 17~92$^{\Delta/\Delta}$ CD4^{+} T cells transfected with *Hif1a* 3′UTR luciferase reporters together with miR-17~92 miRNA mimics or Ctl mimic as described in C. (**G**) Renilla luciferase activity in primary 17~92+/+ control and miR-17~92-deficient CD4^{+} T cells transfected with position 1 (P1) of *Rora* 3′UTR luciferase reporters (see methods) together with miR-18a mimic or control miRNA mimics (Ctl mimic), as described in C. (**H, I**) Frequencies of CCR6^{+}RORγt^{+} cells from 17~92$^{+/+}$ control (circles), 17~92$^{\Delta/\Delta}$ (triangles), and 17~92$^{\Delta/\Delta}$*Rora*$^{sg/+}$ (squares) (**H**) or 17~92$^{\Delta/\Delta}$*Smad4*$^{\Delta/+}$ (squares) (**I**) cells after 3.5 days of *in vitro* culture under Th17-polarizing conditions with varying doses of TGFβ, as assessed by flow cytometry. *P<0.05, **P<0.01, ***P<0.001 (one-tailed paired *t*-test; (**B, D, E**) or one-way ANOVA with Dunnett's post-test (comparing each column to 17~92$^{\Delta/\Delta}$ + Ctl mimic mean; (**C, F, G**)) or two-way ANOVA with Bonferroni post-test (comparing 17~92$^{\Delta/\Delta}$ and 17~92$^{\Delta/\Delta}$*Rora*$^{sg/+}$ (**H**) or 17~92$^{\Delta/\Delta}$ and 17~92$^{\Delta/\Delta}$*Smad4*$^{\Delta/+}$ (**I**)). Data are pooled from six independent experiments (**B, D** (left)) or two to four independent experiments (**C, D** (right), **E-I**) with one to two mice per genotype (mean and s.e.m; **A-I**).